

An Umpolung Approach to Acyclic 1,4-Dicarbonyl Amides via Photoredox-Generated Carbamoyl Radicals

Jason D. Williams,^[a, b, c] Stuart G. Leach,^{*,[b]} and William J. Kerr^{*,[a]}

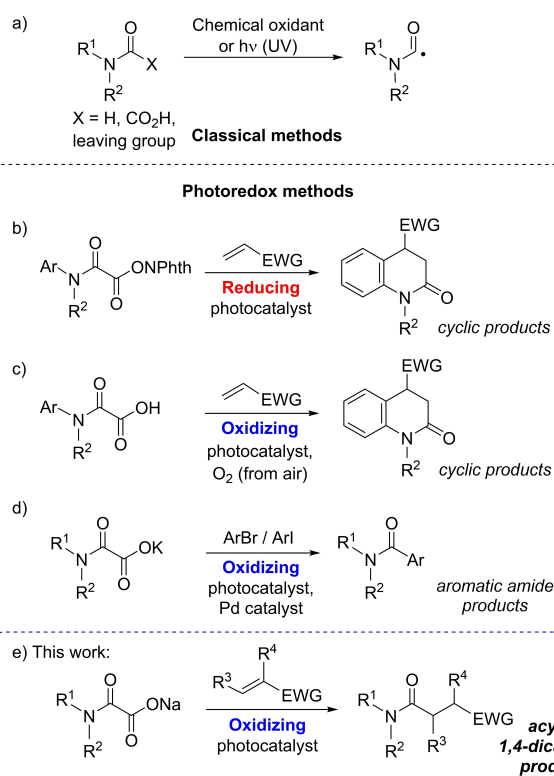
Abstract: A method for the generation and reaction of carbamoyl radicals from oxamate salts, followed by reaction with electron-poor olefins, is described. The oxamate salt acts as a reductive quencher in the photoredox catalytic cycle, allowing mild and mass-efficient formation of 1,4-dicarbonyl products; a challenging transformation in the context of functionalized amide formation. Increased understanding has

been obtained by the use of ab initio calculations, in support of experimental observations. Furthermore, steps have been taken towards an environmentally-friendly protocol, by utilizing sodium as a cheap and low mass counterion, and demonstrating successful reactions using a metal-free photocatalyst and a sustainable, non-toxic solvent system.

Introduction

The advent of photoredox and electrochemical methods has driven a resurgence in the creation of synthetically useful strategies involving single-electron processes, due to the mild and gradual release of these highly reactive species.^[1] Although a wide range of radical species have been generated via photoredox methodologies (e.g. alkyl,^[2] aryl,^[2b,3] acyl,^[4] and various *N*-centered^[5] radicals), carbamoyl radicals appear to have received considerably less attention.^[6]

A range of classical methods for the generation of carbamoyl radicals has been disclosed, from a variety of precursors, by chemical means^[7] or UV light initiation^[8] (Scheme 1a). The relative harshness of these procedures for radical generation has limited the synthetic utility of carbamoyl radicals, for the most part, to simple cyclization reactions. More specifically, intermolecular reactions have been demonstrated in only a few cases, and are restricted to relatively unfunctionalized molecules.^[9] Having stated this, recent advances from



Scheme 1. Methods of carbamoyl radical formation: a) classical methods using a chemical oxidant or UV light; b) photoredox reduction of an oxamic acid, activated as an *N*-hydroxyphthalimide; c) photoredox oxidation of a latent oxamic acid followed by cyclization; d) photoredox oxidation of a potassium oxamate salt, followed by Pd-catalyzed cross-coupling; e) photoredox oxidation of sodium oxamate salts, followed by addition to electron-poor olefins (*this work*).

Melchiorre and co-workers have led to the exploitation of carbamoyl radicals in Giese-type reactions,^[10] starting from carbamoyl chlorides, and in Ni-catalyzed couplings with aryl bromides, from more complex dihydropyridine-based carbamoyl radical precursors.^[11]

[a] Dr. J. D. Williams, Prof. Dr. W. J. Kerr
Department of Pure and Applied Chemistry
University of Strathclyde
295 Cathedral Street, Glasgow, G1 1XL (UK)
E-mail: w.kerr@strath.ac.uk

[b] Dr. J. D. Williams, Dr. S. G. Leach
API Chemistry, GlaxoSmithKline
Medicines Research Centre
Gunnels Wood Road, Stevenage, Hertfordshire, SG1 2NY (UK)
E-mail: stuart.g.leach@gsk.com

[c] Dr. J. D. Williams
Present address: Center for Continuous Flow Synthesis and Processing (CC FLOW)
Research Center Pharmaceutical Engineering GmbH (RCPE)
Inffeldgasse 13, 8010 Graz (Austria)

Supporting information for this article is available on the WWW under <https://doi.org/10.1002/chem.202300403>

© 2023 The Authors. Chemistry - A European Journal published by Wiley-VCH GmbH. This is an open access article under the terms of the Creative Commons Attribution License, which permits use, distribution and reproduction in any medium, provided the original work is properly cited.

In recent reports, carbamoyl radicals have been generated using photoredox chemistry, in both reductive and oxidative quenching cycles. For example, Donald and co-workers described the reduction of aryl *N*-hydroxyphthalimido oxamides using the strongly reducing catalyst, Ir(ppy)₃.^[12] The resulting carbamoyl radical undergoes a process including homolytic aromatic substitution, forming 3,4-dihydroquinolin-2-ones (Scheme 1b). The required substrate prefunctionalization, however, is mass- and step-inefficient, and the starting oxamides are described as unstable to silica gel.

Conversely, oxamic acid starting materials, or their oxamate salts, require no prefunctionalization, carry little unused mass, and are readily handled. Carbamoyl radical generation by oxidation of these species has been demonstrated via two distinct approaches. Feng and co-workers disclosed a transformation which also furnishes 3,4-dihydroquinolin-2-ones, but from the latent oxamic acid starting material, using the strongly oxidizing Ir[dF(CF₃)ppy]₂(dtbbpy)PF₆ photocatalyst (Scheme 1c).^[13] In this case, the proposed mechanism requires oxygen as an external oxidant to mediate the catalytic cycle, due to the absence of any oxidizing species along the reactive pathway. In a similar approach, use of an external hypervalent iodine or persulfate oxidant to form carbamoyl radicals for reaction with heteroaromatics has also been reported recently.^[14]

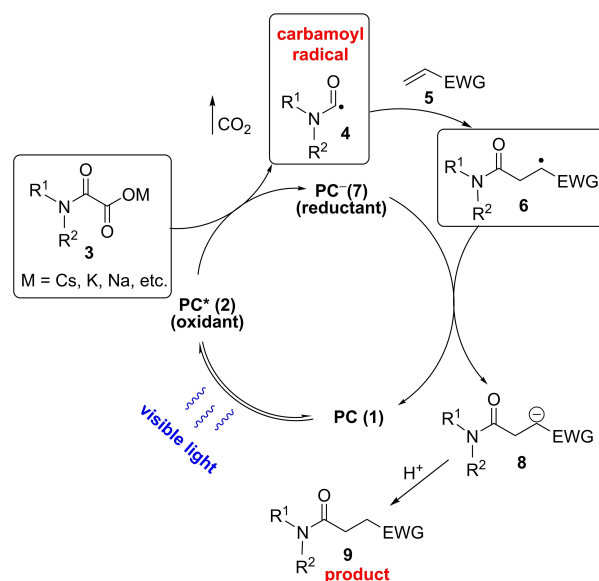
Separately, Fu and co-workers utilized the corresponding potassium oxamate salts in a palladium/photoredox dual catalysis procedure, coupling the resultant carbamoyl radicals with various (hetero)aryl bromides and iodides (Scheme 1d).^[15] This approach utilized the same oxidatively active iridium catalyst as employed within the Feng system, and showed good functional group tolerance across a range of (hetero)aromatic amides. The process is, however, limited to the synthesis of aromatic amide products.

Thus far, these methodologies do not appear to have fully realized the potential of carbamoyl radicals as an almost unique umpolung case^[16] whereby the amide carbonyl unit becomes nucleophilic. Conceptually, this approach has the potential to allow access to 1,4-dicarbonyls through 1,4-addition to an α,β -unsaturated electrophile. Although the 1,4-dicarbonyl motif is readily accessible for some functional groups (aldehydes through the Stetter reaction,^[17] for example), the equivalent transformation for amides has scarcely been reported^[18] and, to the best of our knowledge, in only a very limited number of examples using a photoredox approach.^[10,11b] Since the 1,4-dicarbonyl unit represents a particularly useful motif in heterocycle formation, and for access to medicinally-relevant compounds in general, a practical and effective method for their generation is considered highly desirable. Herein we report the development of a facile protocol for the generation of carbamoyl radicals from metal oxamate salts, and their reaction with electron-deficient olefins to furnish linear amide products bearing this valuable 1,4-dicarbonyl motif (Scheme 1e).

Results and Discussion

We sought to utilize a conceptually simple redox-neutral photoredox catalytic cycle (Scheme 2), in which the excited state photocatalyst **2** is reductively quenched by the oxamate metal salt **3**, which would, in turn, undergo decarboxylation to afford the carbamoyl radical **4**. This nucleophilic carbamoyl radical would then add to electron-poor olefin **5**, generating the stabilized radical species **6**. This intermediate then receives an electron from the reduced state photocatalyst **7**, forming anionic species **8**, which yields the desired product **9** upon protonation. This type of redox-neutral cycle was proposed to be achievable based on the relatively low oxidation potential of oxamate metal salts **3** (approx. +1.24 V vs SCE in DMF for an *N*-alkyl oxamate, and +1.30 V vs SCE in DMF for an *N*-aryl oxamate; see Supporting Information, Table S1). These potentials are accessible by a broad range of organic and metal-based photoredox catalysts.^[1b,d] The corresponding reduction of stabilized radical **6** is also proposed to be relatively facile, with a calculated potential of between -0.63 V and -0.72 V (vs SCE).^[19]

This proposed mechanism was examined in more detail using DFT calculations, in order to verify that all required transition states and intermediates were feasible (Figure 1). The oxamate anion **3a'** and ground state PC1 were taken as the overall ground state energy; however, oxidation and reduction transition state energies could not be found, due to the large size of the catalyst species. Nonetheless, the energy of the reduced state photocatalyst PC1' with its oxidized oxamate partner **3a''** was calculated to be 56.8 kcal mol⁻¹ higher in energy; a value lower than the energy of a photon absorbed at 440 nm (64.5 kcal mol⁻¹), the lower energy range of photons absorbed by PC1 (see Supporting Information, Figure S1). These relative energies reinforced our proposal that the initial



Scheme 2. Proposed mechanism for redox neutral photoredox catalytic cycle.

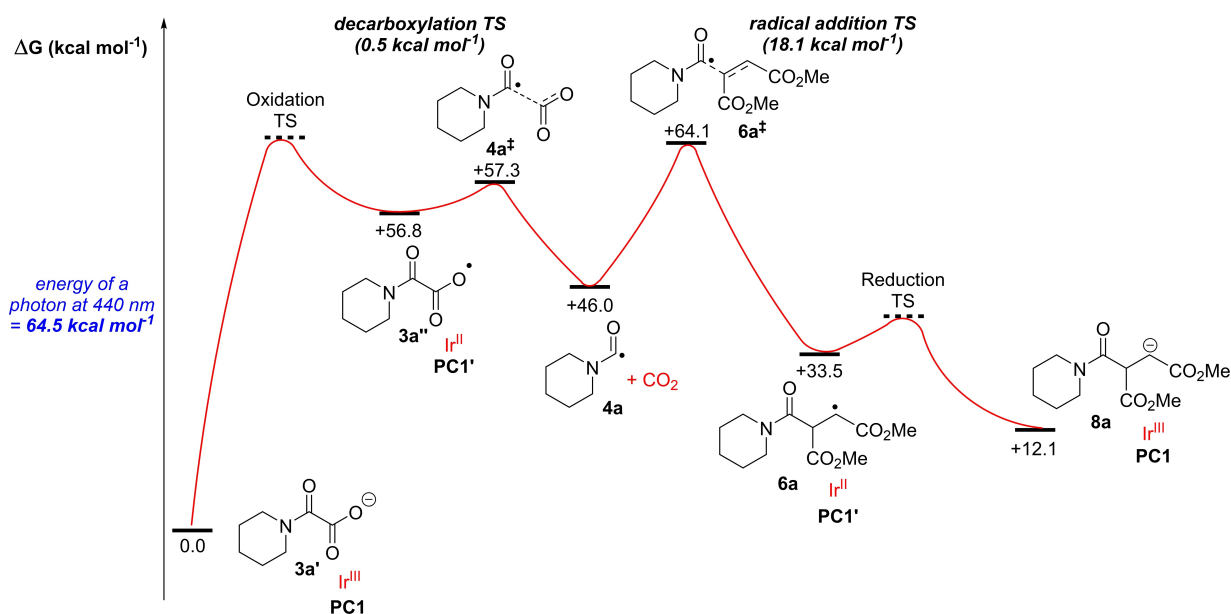


Figure 1. DFT assessment of the proposed reaction pathway (see Scheme 2). Energies were calculated using UB3LYP/6-31G(d,p).

oxidation event would, indeed, be feasible. Following this oxidation, the oxamate radical undergoes a *pseudo*-barrierless decarboxylation ($0.5 \text{ kcal mol}^{-1}$ energy barrier) to form the significantly more stable carbamoyl radical **4a**. The subsequent radical addition to acceptor dimethyl fumarate **5a** has an energy barrier of $18.1 \text{ kcal mol}^{-1}$, which can be overcome at room temperature. Following reduction by the photocatalyst **PC1'**, the stabilized anion **8a** is formed, which simply requires protonation to form the desired product **9a**. All of the calculated transition states and intermediate energies were deemed accessible, and there is a general downward energy trend, supporting the initial mechanistic proposal (Scheme 2).

With a mechanistic hypothesis, supported by DFT calculations, in hand, our proof of concept and optimization studies began, starting from conditions based on a related transformation,^[20] whilst attempting to select a photoredox catalyst with the desired balance of oxidation and reduction potential (Figure 2; also see Supporting Information, Table S2–3). Gratifyingly, using the conditions in Table 1, entry 1, photocatalyst **PC1** delivered an 89% yield of product **9a** in the reaction of piperidine oxamate salt **3a** with dimethyl fumarate **5a**. In addition, we also wanted to explore the use of an effective organic photoredox catalysts, for reasons of cost and sustainability. Accordingly, further catalyst screening employed the simple dicyanoanthracene catalyst **PC2**, which led to a low level of product formation (Table 1, entry 2). Both **PC3** and **PC4** have been shown to be effective organic surrogates for **PC1**,^[21] and so were examined in this transformation. Pleasingly, the acridinium catalyst **PC3** showed a good level of conversion to the desired product (Table 1, entry 3); in contrast, **PC4** proved to be largely ineffective in this transformation (Table 1, entry 4). Based on the pertinent goal of replacing metals in photoredox catalysis, we planned to revisit the use of **PC3** once the method using **PC1** had been fully explored.

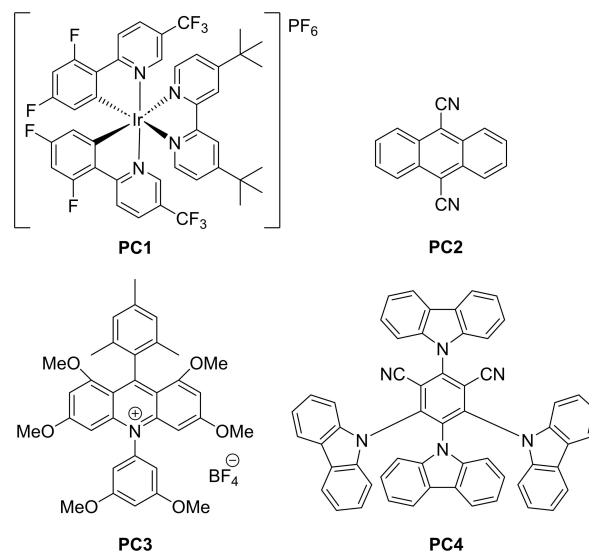
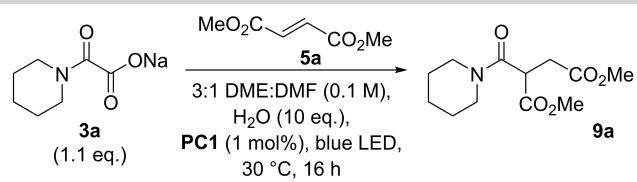


Figure 2. Structure of photoredox catalysts **PC1**–**PC4**; see Table 1.

The use of salts of the oxamate starting material was viewed to be advantageous, when compared to the latent oxamic acid. These oxamate salts are more routinely prepared and isolated, as they do not require acidification after basic hydrolysis of the corresponding methyl ester, and any organic impurities can easily be removed by washing with organic solvents. Furthermore, their handling is also favorable, due to their physical form as free flowing solids. Depending upon the identity of the cation, these salts are hygroscopic to varying extents. However, when stored in a dry environment, or dried prior to use, this has no effect on reaction performance, and no degradation of the oxamate salts has been observed over the course of at least three months.

Table 1. Selected results from reaction optimization studies.^[a]



Entry	Deviation from standard conditions	Yield 9a [%] ^[b]	Remaining 5a [%] ^[b]
1	None	89	3
2	PC2 (2 mol%) in place of PC1	25	31
3	PC3 (2 mol%) in place of PC1	78	6
4	PC4 (2 mol%) in place of PC1	23	44
5	K salt in place of Na salt	87	0
6	Cs salt in place of Na salt	87	0
7	NBu ₄ salt in place of Na salt	52	44
8	No water added	37	46
9	56 equiv. water (10% vol.) added	71	0
10	DCM in place of DME:DMF	22	18
11	Acetonitrile in place of DME:DMF	44	6
12	Acetone in place of DME:DMF	80	2
13	1 equiv. 3a in place of 1.1 equiv.	82	7
14	2 mol% PC1 in place of 1 mol%	78	12
15	0.5 mol% PC1 in place of 1 mol%	85	7
16	0.2 M concentration	53	36
17	0.05 M concentration	77	0
18 ^[c]	Absence of light	0	> 95
19 ^[c]	Absence of photocatalyst	0	> 95
20 ^[c]	2 equiv. TEMPO added	0	> 95

^[a] Reactions were performed on 0.1 mmol scale (1 mL), using 1.1 equiv. **3a** and 1.0 equiv. **5a**. The reactions were irradiated by 1×blue LED lamp for 16 h. ^[b] Determined by HPLC analysis, using biphenyl as an internal standard. ^[c] Control reactions were carried out in acetone using methylenedihydrofuran-2(3H)-one as the olefin coupling partner **5g**, in place of **5a**.

It had been anticipated that the identity of the oxamate cation may play a role in determining the reaction performance. Accordingly, various alternative salts were examined under the standard reaction conditions (see Supporting Information, Table S4). Group one metals appeared to give the best reaction performance (Table 1, entries 1, 4, and 5). It was also envisaged that a tetrabutylammonium counterion would result in a homogeneous reaction solution, further boosting reaction efficiency. Surprisingly, this change was found to have a detrimental effect, with a lower conversion observed in this case than any other counterion examined (Table 1, entry 7).

Further examining the reaction component solubility, the influence of water was determined, as this was expected to have significant impact upon the proportion of reaction components in solution versus the solid phase (see Supporting Information, Table S5). A low fraction of water (10 equivalents, Table 1, entry 1) gave optimal reactivity, and it was found that removing this water completely was highly detrimental (Table 1, entry 8). Conversely, the presence of additional water was also detrimental to the reaction performance (Table 1, entry 9). This implies that there are complex requirements for the

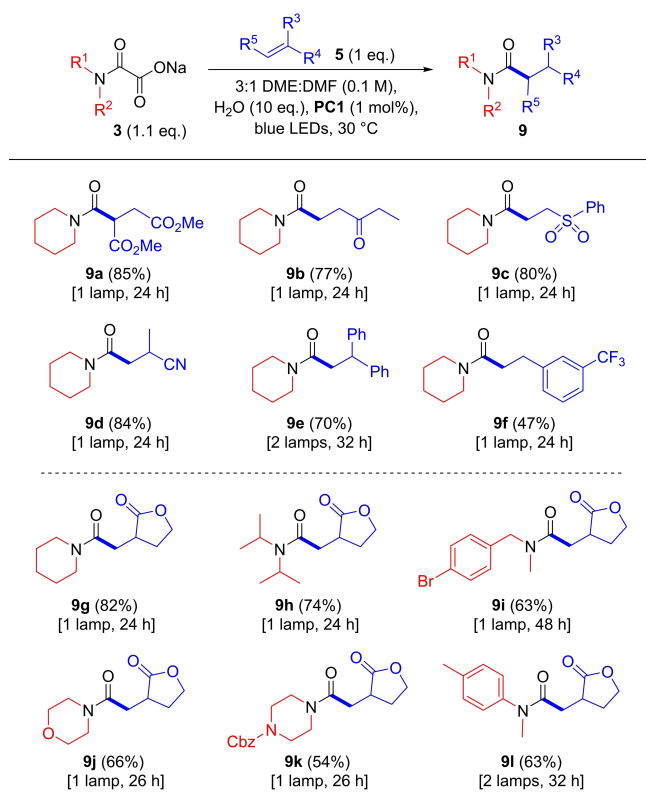
reaction medium, in which a small proportion of water is required to solubilize the oxamate salt starting material, yet the presence of water in larger quantities is disfavored. Coupled with the observation that the NBu₄ cation (the only fully soluble oxamate salt) displayed the poorest reactivity, this suggests that surface effects may be important for effective oxidation of the oxamate starting material.

Subsequently, attempts were made to optimize the solvent used for this reaction, through screening a range of distinct solvent classes (see Supporting Information, Table S6). Despite success in related work,^[13] dichloromethane proved to be a poor choice in this case (Table 1, entry 10). Additionally, acetonitrile, a common choice for many radical reactions, also led to reduced performance (Table 1, entry 11). Surprisingly, though, use of the environmentally-benign solvent, acetone, resulted in a conversion similar to the optimal conditions (Table 1, entry 12). This observation will also be further explored and discussed, with the aim of achieving a safer and more sustainable transformation.

Whilst a slight excess of oxamate reagent was shown to be beneficial (Table 1, entry 1 vs. 13), the proportion of this substrate was not increased further based on a desire to avoid an uneconomical excess of reagents. Unfortunately, attempts to improve reaction performance and throughput by altering catalyst loading and concentration yielded less favorable outcomes, when either increasing or decreasing these variables (Table 1, entry 14–17). Finally, control reactions were performed, in order to corroborate the proposed reaction mechanism (Table 1, entries 18–20). The absence of either light or photocatalyst both led to no formation of the desired product, confirming that the reaction is proceeding under photocatalytic conditions. Furthermore, the addition of TEMPO, as a radical inhibitor, also led to no formation of the desired product, further supporting the proposal that a radical reaction mechanism is in operation.

Using the optimized reaction conditions, the substrate tolerance of the transformation was explored (Scheme 3). The scope of the olefin reaction component **5** was examined using sodium 2-oxo-2-(piperidin-1-yl)acetate **3a** as the oxamate coupling partner. Using the standard coupling partner from the optimization studies, tertiary amide **9a** was isolated in an excellent 85% yield. Following this, a broad range of other olefin coupling partners were successfully applied, allowing incorporation of ketone (**9b**), sulfone (**9c**) and nitrile (**9d**) functionalities into the resulting tertiary amides, in good yields. Gratifyingly, this protocol could be extended to include styrene coupling partners with some success. Although requiring the use of an additional LED lamp, the common radical trap 1,1-diphenylethylene was incorporated into amide product **9e** in a good 70% yield. Furthermore, amide **9f** was prepared by reaction with 3-(trifluoromethyl)styrene in a reasonable 47% yield, representing an expansion to a new class of reaction partners.

When considering the scope with respect to the oxamate **3** starting material, methylenedihydrofuran-2(3H)-one **5g** was used as the standard olefin coupling partner. Reaction with **3a** yielded amide **9g** in an excellent 82% yield. Substantially



Scheme 3. Substrate scope of the developed reaction conditions in both oxamate and olefin coupling partner. Reactions were performed on 0.4 mmol scale (4 mL), using 1.1 equiv. **3**. The reactions were irradiated by 1 or 2× blue LED lamps for the indicated reaction time. All yields shown are those of isolated products.

increasing the steric hindrance around the oxamate had no significant effect on the reaction yield, as demonstrated by the access to di-*iso*-propylamide **9h** in a good (74%) yield. Furthermore, the formation of product **9i** demonstrates that a benzylic moiety is tolerated in the oxamate, alongside an aromatic bromide, useful for subsequent functionalization. Saturated heterocyclic oxamate substrates were also tolerated, with the morpholine- and piperidine-derived oxamates giving acceptable yields of the corresponding products **9j** and **9k**.

Finally, an aniline-derived oxamate starting material yielded 63% of the desired linear amide **9l**, albeit whilst requiring 2 LED lamps. This result provides a complementary product to previously reported photoredox methods, in which a cyclization, via homolytic aromatic substitution (HAS), is observed following addition to the radical acceptor.^[13,12] Assessment of this possible reaction pathway in our system, using DFT calculations (Figure 3), reveals a relatively low energy barrier to the intramolecular attack of radical intermediate **6l** (16.5 kcal mol⁻¹). However, the resulting radical **6l'** is significantly higher in energy than **6l** (+6.1 kcal mol⁻¹), and we propose that the rapid reduction of **6l** is preferred. In a previous report, using the same photoredox catalyst, the required oxidation of **6l'** to form **9l'** has been justified by the involve-

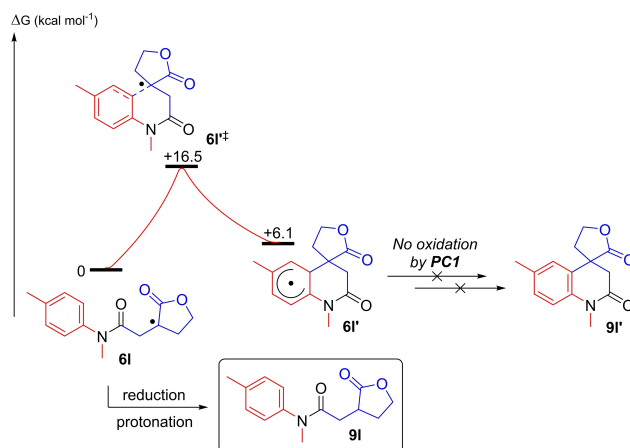


Figure 3. DFT assessment of the possible homolytic aromatic substitution cyclization pathway in the formation of products **9l'** and **9l**. Calculated using UB3LYP/6-31 + G(d,p).

ment of oxygen.^[13] In our system, product **9l'** was observed in only a trace quantity, via mass spectrometry.

Returning to the alkene scope, using **3a** with cyclohex-2-enone **5m** as the coupling partner, to form product **9m**, gave a poor 11% yield. This low reactivity was examined through DFT calculations (Figure 4), comparing this reaction with the successful formation of **9g**. In this case, the comparatively higher (by +3.4 kcal mol⁻¹) barrier to radical addition (**6g[±]** vs. **6m[±]**) is proposed to account for the appreciably lower reaction yield, and can be explained simply by the increased steric hindrance around the site of radical conjugate attack. These outcomes represent a contrast between 1,1- and 1,2-disubstituted alkenes, and could demonstrate a limit to the scope of this process. A more nucleophilic acyl radical is expected to undergo this radical attack more readily, despite the increased steric influence, explaining the compatibility of the more

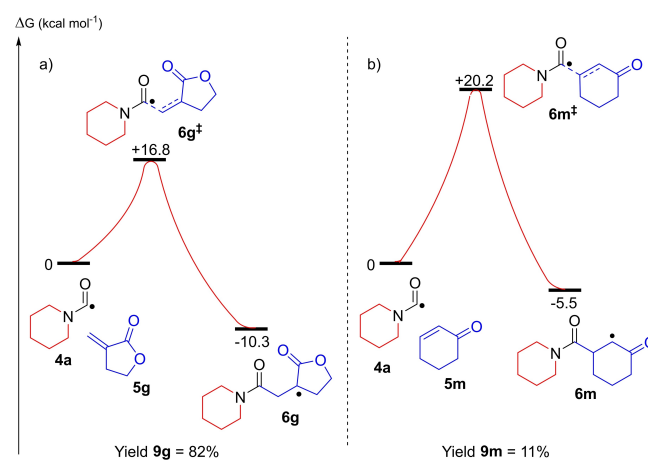
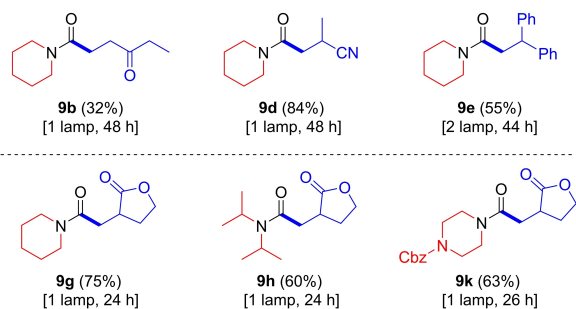
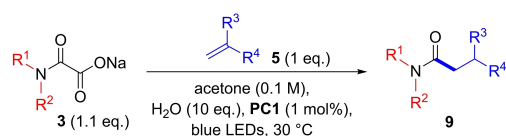


Figure 4. DFT assessment of the lowered effectiveness of reaction with a 1,2-disubstituted alkene to form **9m** versus a 1,1-disubstituted alkene to form **9g**. Calculated using UB3LYP/6-31 + G(d,p).

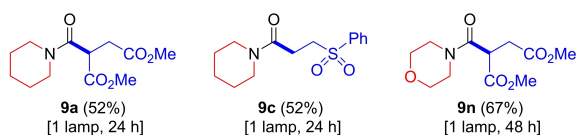
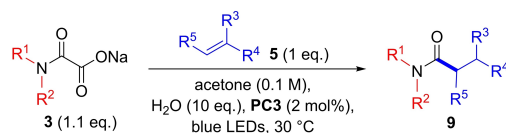
hindered substitution pattern within synthetic methodologies which implement more reactive radical species.^[2a,4b,h,20]

Following exploration of the substrate scope, we returned to efforts to improve the industrial applicability of this transformation. Specifically, we first investigated the implementation of a more sustainable solvent, since both DME and DMF present a notable health risk.^[22] From the initial methodology optimization, acetone was found to be a suitable solvent for these reactions (Table 1, entry 12), and represented a far more desirable solvent from a health and environmental standpoint. Accordingly, several reactions from the initial substrate scope were re-examined under these conditions, with 10 equiv. of added water, as previously found to be optimal in the DME:DMF system (Scheme 4).

Using acetone as solvent, the yields achieved tended to be somewhat lower than in the DME:DMF solvent system. In some cases, this could be accounted for by attack of a reaction intermediate into a molecule of reaction solvent. For example,



Scheme 4. Substrate scope of the developed reaction using acetone as a solvent in both oxamate and olefin coupling partner. Reactions were performed on 0.4 mmol scale (4 mL), using 1.1 equiv. **3**. The reactions were irradiated by 1 or 2× blue LED lamps for the indicated reaction time. All yields shown are those of isolated products.



Scheme 5. Substrate scope of the developed reaction using organic photocatalyst **PC3** and acetone as a solvent. Reactions were performed on 0.4 mmol scale (4 mL), using 1.1 equiv. **3**. The reactions were irradiated by 1× blue LED lamp for the indicated reaction time. All yields shown are those of isolated products.

nitrile-containing product **9d** was, again, isolated in good yield, with 4% of a by-product, arising from reaction of an intermediate with an acetone unit (**9d'**, see Supporting Information), also being isolated. Products **9e**, **9g** and **9h** were also isolated in slightly lower yields than the initially developed conditions; however, product **9k** was obtained in an increased yield within this solvent system.

To further improve the preparative suitability of this procedure, we re-visited the use of organic photocatalyst **PC3**, which had performed well in the initial optimization studies. Using this catalyst, products **9a**, **9c**, and **9n** were isolated in good yields (Scheme 5). It should be noted that the organic catalyst system and reaction conditions were not subjected to a full optimization process, and iridium catalyst **PC1** is considered to be more broadly effective for the coupling system developed as part of this study. However, where a single product is required, particularly as part of a scaled up process (rather than substrate diversity), the organic photocatalyst could potentially be tuned to the specific substrate(s) in order to provide more optimal yields of the desired product.^[21a] Nonetheless, this brief latter substrate study demonstrates the possibility of carrying out transformations under transition metal-free conditions, further enhancing the profile of this protocol as a sustainable methodology.

Conclusion

We have demonstrated an efficient synthesis of acyclic tertiary amides by photoredox generation of carbamoyl radicals, followed by radical attack on an alkene species. This represents a mild and atom-efficient methodology, which achieves an uncommon umpolung disconnection of 1,4-dicarbonyls containing an amide unit. The overall approach, reaction mechanism, and rationalization of multiple experimental observations have been supported by the use of associated DFT calculations. Additionally, the application of more sustainable and industrially-relevant reaction conditions has also been successfully advanced, further emphasizing the synthetic potential of this photoredox methodology.

Experimental Section

See the Supporting Information for all experimental procedures, compound characterization, and details of the DFT calculations.

Acknowledgements

The authors would like to thank Dr David M. Lindsay for assistance in manuscript preparation, alongside Mr Lee J. Edwards and Dr Blandine McKay for assistance with the photochemical equipment, and Dr Colin M. Edge for guidance in performing DFT calculations. J. D. W. would also like to thank GlaxoSmithKline for financial support.

Conflict of Interest

The authors declare no conflict of interest.

Data Availability Statement

The data that support the findings of this study are available in the supplementary material of this article.

Keywords: amides · photochemistry · photoredox catalysis · radical reactions · synthetic methods

- [1] a) M. H. Shaw, J. Twilton, D. W. C. MacMillan, *J. Org. Chem.* **2016**, *81*, 6898–6926; b) C. K. Prier, D. A. Rankic, D. W. C. MacMillan, *Chem. Rev.* **2013**, *113*, 5322–5363; c) J. K. Matsui, S. B. Lang, D. R. Heitz, G. A. Molander, *ACS Catal.* **2017**, *7*, 2563–2575; d) N. A. Romero, D. A. Nicewicz, *Chem. Rev.* **2016**, *116*, 10075–10166; e) M. Yan, Y. Kawamata, P. S. Baran, *Chem. Rev.* **2017**, *117*, 13230–13319.
- [2] a) H. Huo, K. Harms, E. Meggers, *J. Am. Chem. Soc.* **2016**, *138*, 6936–6939; b) J.-P. Goddard, C. Ollivier, L. Fensterbank, *Acc. Chem. Res.* **2016**, *49*, 1924–1936.
- [3] a) Y. Iwata, Y. Tanaka, S. Kubosaki, T. Morita, Y. Yoshimi, *Chem. Commun.* **2018**, *54*, 1257–1260; b) C.-S. Wang, P. H. Dixneuf, J.-F. Soulé, *Chem. Rev.* **2018**, *118*, 7532–7585.
- [4] a) G. Bergonzini, C. Cassani, C.-J. Wallentin, *Angew. Chem. Int. Ed.* **2015**, *54*, 14066–14069; *Angew. Chem.* **2015**, *127*, 14272–14275; b) L. Capaldo, R. Riccardi, D. Ravelli, M. Fagnoni, *ACS Catal.* **2018**, *8*, 304–309; c) J. Liu, Q. Liu, H. Yi, C. Qin, R. Bai, X. Qi, Y. Lan, A. Lei, *Angew. Chem. Int. Ed.* **2014**, *53*, 502–506; *Angew. Chem.* **2014**, *126*, 512–516; d) G. Bergonzini, C. Cassani, H. Lorimer-Olsson, J. Hörberg, C.-J. Wallentin, *Chem. Eur. J.* **2016**, *22*, 3292–3295; e) R. Ruzi, M. Zhang, K. Ablajan, C. Zhu, *J. Org. Chem.* **2017**, *82*, 12834–12839; f) C.-G. Li, G.-Q. Xu, P.-F. Xu, *Org. Lett.* **2017**, *19*, 512–515; g) C. Zhou, P. Li, X. Zhu, L. Wang, *Org. Lett.* **2015**, *17*, 6198–6201; h) G.-Z. Wang, R. Shang, W.-M. Cheng, Y. Fu, *Org. Lett.* **2015**, *17*, 4830–4833; i) Y. Liu, Q.-L. Wang, C.-S. Zhou, B.-Q. Xiong, P.-L. Zhang, C. Yang, K.-W. Tang, *J. Org. Chem.* **2018**, *83*, 2210–2218.
- [5] a) M. D. Kärkäs, *ACS Catal.* **2017**, *7*, 4999–5022; b) J.-R. Chen, X.-Q. Hu, L.-Q. Lu, W.-J. Xiao, *Chem. Soc. Rev.* **2016**, *45*, 2044–2056; c) D. F. Reina, E. M. Dauncey, S. P. Morcillo, T. D. Svejstrup, M. V. Popescu, J. J. Douglas, N. S. Sheikh, D. Leonori, *Eur. J. Org. Chem.* **2017**, *2017*, 2108–2111; d) C. Pratley, S. Fenner, J. A. Murphy, *Chem. Rev.* **2022**, *122*, 8181–8260.
- [6] Reports on the use of carbamoyl radicals are discussed, within broader coverage, in the following reviews: a) C. Chatgililoglu, D. Crich, M. Komatsu, I. Ryu, *Chem. Rev.* **1999**, *99*, 1991–2070; b) C. Raviola, S. Protti, D. Ravelli, M. Fagnoni, *Green Chem.* **2019**, *21*, 748–764; c) F. Penteado, E. F. Lopes, D. Alves, G. Perin, R. G. Jacob, E. J. Lenardão, *Chem. Rev.* **2019**, *119*, 7113–7278.
- [7] a) A. F. Bella, L. V. Jackson, J. C. Walton, *Org. Biomol. Chem.* **2004**, *2*, 421–428; b) A. F. Bella, A. M. Z. Slawin, J. C. Walton, *J. Org. Chem.* **2004**, *69*, 5926–5933; c) L. Benati, G. Bencivenni, R. Leardini, M. Minozzi, D. Nanni, R. Scialpi, P. Spagnolo, G. Zanardi, *J. Org. Chem.* **2006**, *71*, 3192–3197; d) J. H. Rigby, D. M. Danca, J. H. Horner, *Tetrahedron Lett.* **1998**, *39*, 8413–8416; e) F. Minisci, F. Coppa, F. Fontana, *J. Chem. Soc. Chem. Commun.* **1994**, 679–679. For more contemporary use of a quinolinone organic photocatalyst for visible light induced generation of an ethoxy radical, which, in turn, abstracts a hydrogen atom from formamides to form a carbamoyl radical, see: f) I. Kim, G. Kang, K. Lee, B. Park, D. Kang, H. Jung, Y.-T. He, M.-H. Baik, S. Hong, *J. Am. Chem. Soc.* **2019**, *141*, 9239–9248.
- [8] a) J. C. Walton, *Acc. Chem. Res.* **2014**, *47*, 1406–1416; b) G. Pattenden, S. J. Reynolds, *J. Chem. Soc. Perkin Trans. 1* **1994**, 379–385; c) E. M. Scanlan, J. C. Walton, *Chem. Commun.* **2002**, 2086–2087.
- [9] a) G. P. Gardini, F. Minisci, G. Palla, A. Arnone, R. Galli, *Tetrahedron Lett.* **1971**, *12*, 59–62; b) F. Minisci, F. Fontana, F. Coppa, Y. M. Yan, *J. Org. Chem.* **1995**, *60*, 5430–5433; c) V. G. Correia, J. C. Abreu, C. A. E. Barata, L. H. Andrade, *Org. Lett.* **2017**, *19*, 1060–1063.
- [10] E. de Pedro Beato, D. Mazzarella, M. Balletti, P. Melchiorre, *Chem. Sci.* **2020**, *11*, 6312–6324.
- [11] a) N. Alandini, L. Buzzetti, G. Favi, T. Schulte, L. Candish, K. D. Collins, P. Melchiorre, *Angew. Chem. Int. Ed.* **2020**, *59*, 5248–5253; *Angew. Chem.* **2020**, *132*, 5286–5291; for further reactions from carbamoyl radicals generated from Hantzsch esters, see: Giese-type reactions: b) L. Cardinale, M. O. Konev, A. J. van Wengelin, *Chem. Eur. J.* **2020**, *26*, 8239–8243; addition to pyridines: c) I. Kim, S. Park, S. Hong, *Org. Lett.* **2020**, *22*, 8730–8734.
- [12] a) W. F. Petersen, R. J. K. Taylor, J. R. Donald, *Org. Lett.* **2017**, *19*, 874–877; b) W. F. Petersen, R. J. K. Taylor, J. R. Donald, *Org. Biomol. Chem.* **2017**, *15*, 5831–5845.
- [13] Q.-F. Bai, C. Jin, J.-Y. He, G. Feng, *Org. Lett.* **2018**, *20*, 2172–2175.
- [14] a) A. H. Jatoi, G. G. Pawar, F. Robert, Y. Landais, *Chem. Commun.* **2019**, *55*, 466–469; b) M. Jouffroy, J. Kong, *Chem. Eur. J.* **2019**, *25*, 2217–2221.
- [15] W.-M. Cheng, R. Shang, H.-Z. Yu, Y. Fu, *Chem. Eur. J.* **2015**, *21*, 13191–13195.
- [16] a) M. A. Ganiek, M. R. Becker, G. Berionni, H. Zipse, P. Knochel, *Chem. Eur. J.* **2017**, *23*, 10280–10284; b) A. Nagaki, Y. Takahashi, J.-I. Yoshida, *Angew. Chem. Int. Ed.* **2016**, *55*, 5327–5331; *Angew. Chem.* **2016**, *128*, 5413–5417.
- [17] a) H. Stetter, *Angew. Chem. Int. Ed. Engl.* **1976**, *15*, 639–647; b) X. Bugaut, F. Glorius, *Chem. Soc. Rev.* **2012**, *41*, 3511–3522; c) S. R. Yetra, A. Patra, A. T. Biju, *Synthesis* **2015**, *47*, 1357–1378; d) D. M. Flanagan, F. Romanov-Michailidis, N. A. White, T. Rovic, *Chem. Rev.* **2015**, *115*, 9307–9387.
- [18] a) D. Kaiser, C. J. Teskey, P. Adler, N. Maulide, *J. Am. Chem. Soc.* **2017**, *139*, 16040–16043; b) D. Kaldre, I. Klose, N. Maulide, *Science* **2018**, *361*, 664–667.
- [19] N. Bortolamei, A. A. Isse, A. Gennaro, *Electrochim. Acta* **2010**, *55*, 8312–8318.
- [20] C. C. Nawrat, C. R. Jamison, Y. Slutskyy, D. W. C. MacMillan, L. E. Overman, *J. Am. Chem. Soc.* **2015**, *137*, 11270–11273.
- [21] a) A. Joshi-Pangu, F. Lévesque, H. G. Roth, S. F. Oliver, L. C. Campeau, D. Nicewicz, D. A. DiRocco, *J. Org. Chem.* **2016**, *81*, 7244–7249; b) E. Speckmeier, T. G. Fischer, K. Zietler, *J. Am. Chem. Soc.* **2018**, *140*, 15353–15365.
- [22] a) D. Prat, A. Wells, J. Hayler, H. Sneddon, C. R. McElroy, S. Abou-Shehada, P. J. Dunn, *Green Chem.* **2016**, *18*, 288–296; b) A. Jordan, C. G. J. Hall, L. R. Thorp, H. F. Sneddon, *Chem. Rev.* **2022**, *122*, 6749–6794.

Manuscript received: February 7, 2023
Accepted manuscript online: March 2, 2023
Version of record online: March 31, 2023